Plastic lab-on-a-chip for fluorescence excitation with integrated organic semiconductor lasers

Christoph Vannahme,[1,2,*] Sönke Klinkhammer,[2,1] Uli Lemmer,[2] and Timo Mappes[1]

[1] *Institute of Microstructure Technology (IMT), Karlsruhe Institute of Technology (KIT), 76128 Karlsruhe, Germany*
[2] *Light Technology Institute (LTI), Karlsruhe Institute of Technology (KIT), 76128 Karlsruhe, Germany*
**christoph.vannahme@kit.edu*

Abstract: Laser light excitation of fluorescent markers offers highly sensitive and specific analysis for bio-medical or chemical analysis. To profit from these advantages for applications in the field or at the point-of-care, a plastic lab-on-a-chip with integrated organic semiconductor lasers is presented here. First order distributed feedback lasers based on the organic semiconductor tris(8-hydroxyquinoline) aluminum (Alq_3) doped with the laser dye 4-dicyanomethylene-2-methyl-6-(p-dimethylaminostyril)-4H-pyrane (DCM), deep ultraviolet induced waveguides, and a nanostructured microfluidic channel are integrated into a poly(methyl methacrylate) (PMMA) substrate. A simple and parallel fabrication process is used comprising thermal imprint, DUV exposure, evaporation of the laser material, and sealing by thermal bonding. The excitation of two fluorescent marker model systems including labeled antibodies with light emitted by integrated lasers is demonstrated.

OCIS codes: (140.3490) Lasers, distributed-feedback; (140.7300) Visible lasers; (130.3120) Integrated optics devices; (280.3420) Laser sensors.

References and links

1. D. Janasek, J. Franzke, and A. Manz, "Scaling and the design of miniaturized chemical-analysis systems," Nature **442**(7101), 374–380 (2006).
2. P. S. Dittrich, K. Tachikawa, and A. Manz, "Micro total analysis systems. Latest advancements and trends," Anal. Chem. **78**(12), 3887–3908 (2006).
3. F. B. Myers, and L. P. Lee, "Innovations in optical microfluidic technologies for point-of-care diagnostics," Lab Chip **8**(12), 2015–2031 (2008).
4. K. B. Mogensen, and J. P. Kutter, "Optical detection in microfluidic systems," Electrophoresis **30**(S1), S92–S100 (2009).
5. B. Kuswandi, J. Nuriman, J. Huskens, and W. Verboom, "Optical sensing systems for microfluidic devices: a review," Anal. Chim. Acta **601**(2), 141–155 (2007).
6. S. Balslev, A. M. Jorgensen, B. Bilenberg, K. B. Mogensen, D. Snakenborg, O. Geschke, J. P. Kutter, and A. Kristensen, "Lab-on-a-chip with integrated optical transducers," Lab Chip **6**(2), 213–217 (2006).
7. S. Pagliara, A. Camposeo, A. Polini, R. Cingolani, and D. Pisignano, "Electrospun light-emitting nanofibers as excitation source in microfluidic devices," Lab Chip **9**(19), 2851–2856 (2009).
8. M. Ramuz, L. Burgi, R. Stanley, and C. Winnewisser, "Coupling light from an organic light emitting diode (OLED) into a single-mode waveguide: Toward monolithically integrated optical sensors," J. Appl. Phys. **105**(8), 084508 (2009).
9. S. Vengasandra, Y. Cai, D. Grewell, J. Shinar, and R. Shinar, "Polypropylene CD-organic light-emitting diode biosensing platform," Lab Chip **10**(8), 1051–1056 (2010).
10. M. B. Christiansen, M. Schøler, and A. Kristensen, "Integration of active and passive polymer optics," Opt. Express **15**(7), 3931–3939 (2007).
11. T. Woggon, M. Punke, M. Stroisch, M. Bruendel, M. Schelb, C. Vannahme, T. Mappes, J. Mohr, and U. Lemmer, "Organic semiconductor lasers as integrated light sources for optical sensors," in McGraw-Hill volume on Organic Electronics in Sensors and Biotechnology, J. Shinar and R. Shinar, eds. (McGraw-Hill, New York 2009).
12. C. Vannahme, S. Klinkhammer, M. B. Christiansen, A. Kolew, A. Kristensen, U. Lemmer, and T. Mappes, "All-polymer organic semiconductor laser chips: parallel fabrication and encapsulation," Opt. Express **18**(24), 24881–24887 (2010).
13. C. Vannahme, S. Klinkhammer, A. Kolew, P.-J. Jakobs, M. Guttmann, S. Dehm, U. Lemmer, and T. Mappes, "Integration of organic semiconductor lasers and single-mode passive waveguides into a PMMA substrate," Microelectron. Eng. **87**(5-8), 693–695 (2010).

#141032 - $15.00 USD Received 12 Jan 2011; revised 16 Feb 2011; accepted 17 Mar 2011; published 14 Apr 2011

14. Y. Ichihashi, P. Henzi, M. Bruendel, J. Mohr, and D. G. Rabus, "Polymer waveguides from alicyclic methacrylate copolymer fabricated by deep-UV exposure," Opt. Lett. **32**(4), 379–381 (2007).
15. S. Riechel, U. Lemmer, J. Feldmann, S. Berleb, A. G. Mückl, W. Brütting, A. Gombert, and V. Wittwer, "Very compact tunable solid-state laser utilizing a thin-film organic semiconductor," Opt. Lett. **26**(9), 593–595 (2001).
16. S. Klinkhammer, T. Woggon, U. Geyer, C. Vannahme, T. Mappes, S. Dehm, and U. Lemmer, "A continuously tunable low-threshold organic semiconductor distributed feedback laser fabricated by rotating shadow mask evaporation," Appl. Phys. B **97**(4), 787–791 (2009).
17. Y. Yang, G. A. Turnbull, and I. D. W. Samuel, "Hybrid optoelectronics: A polymer laser pumped by a nitride light-emitting diode," Appl. Phys. Lett. **92**(16), 163306 (2008).
18. T. Woggon, S. Klinkhammer, and U. Lemmer, "Compact spectroscopy system based on tunable organic semiconductor lasers," Appl. Phys. B **99**(1-2), 47–51 (2010).
19. S. Klinkhammer, T. Woggon, C. Vannahme, T. Mappes, and U. Lemmer, "Optical spectroscopy with organic semiconductor lasers," Proc. SPIE **7722**, 77221I, 77221I-10 (2010).
20. D. Schneider, T. Rabe, T. Riedl, T. Dobbertin, M. Kröger, E. Becker, H.-H. Johannes, W. Kowalsky, T. Weimann, J. Wang, P. Hinze, A. Gerhard, P. Stössel, and H. Vestweber, "An ultraviolet organic thin-film solid-state laser for biomarker applications," Adv. Mater. **17**, 31–34 (2005).
21. T. Mappes, C. Vannahme, M. Schelb, U. Lemmer, and J. Mohr, "Design for optimized coupling of organic semiconductor laser light into polymer waveguides for highly integrated bio-photonic sensors," Microelectron. Eng. **86**(4-6), 1499–1501 (2009).
22. E. M. Conwell, "Modes in optical waveguides formed by diffusion," Appl. Phys. Lett. **23**(6), 328–329 (1973).
23. R. G. Hunsperger, A. Yariv, and A. Lee, "Parallel end-butt coupling for optical integrated circuits," Appl. Opt. **16**(4), 1026–1032 (1977).
24. J. Carroll, J. Whiteaway, and D. Plumb, Distributed feedback semiconductor lasers, IEE Circuits, Devices and Systems Series 10 (The Institution of Electrical Engineers, London, 1998).
25. N. Ganesh, I. D. Block, P. C. Mathias, W. Zhang, E. Chow, V. Malyarchuk, and B. T. Cunningham, "Leaky-mode assisted fluorescence extraction: application to fluorescence enhancement biosensors," Opt. Express **16**(26), 21626–21640 (2008).
26. C. Vannahme, M. B. Christiansen, T. Mappes, and A. Kristensen, "Optofluidic dye laser in a foil," Opt. Express **18**(9), 9280–9285 (2010).
27. M. Schelb, C. Vannahme, A. Welle, S. Lenhert, B. Ross, and T. Mappes, "Fluorescence excitation on monolithically integrated all-polymer chips," J. Biomed. Opt. **15**(4), 041517 (2010).
28. S. Lenhert, F. Brinkmann, T. Laue, S. Walheim, C. Vannahme, S. Klinkhammer, M. Xu, S. Sekula, T. Mappes, T. Schimmel, and H. Fuchs, "Lipid multilayer gratings," Nat. Nanotechnol. **5**(4), 275–279 (2010).
29. R. G. Heideman, and P. V. Lambeck, "Remote opto-chemical sensing with extreme sensitivity: design, fabrication and performance of a pigtailed integrated optical phase-modulated Mach-Zehnder interferometer system," Sens. Actuators B Chem. **61**(1-3), 100–127 (1999).
30. A. M. Armani, R. P. Kulkarni, S. E. Fraser, R. C. Flagan, and K. J. Vahala, "Label-free, single-molecule detection with optical microcavities," Science **317**(5839), 783–787 (2007).
31. C. F. Carlborg, K. B. Gylfason, A. Kaźmierczak, F. Dortu, M. J. Banuls Polo, A. Maquieira Catala, G. M. Kresbach, H. Sohlstrom, T. Moh, L. Vivien, J. Popplewell, G. Ronan, C. A. Barrios, G. Stemme, and W. van der Wijngaart, "A packaged optical slot-waveguide ring resonator sensor array for multiplex label-free assays in labs-on-chips," Lab Chip **10**(3), 281–290 (2010).
32. U. Huebner, R. Boucher, W. Morgenroth, M. Schmidt, and M. Eich, "Fabrication of photonic crystal structures in polymer waveguide material," Microelectron. Eng. **83**(4-9), 1138–1141 (2006).
33. P. S. Nunes, N. A. Mortensen, J. P. Kutter, and K. B. Mogensen, "Photonic crystal resonator integrated in a microfluidic system," Opt. Lett. **33**(14), 1623–1625 (2008).
34. J. Homola, "Surface plasmon resonance sensors for detection of chemical and biological species," Chem. Rev. **108**(2), 462–493 (2008).

1. Introduction

Specific and highly sensitive detection is a key ingredient for the realization of lab-on-a-chip (LOC) systems for screening and bio-medical or chemical point-of-care analysis of fluids [1, 2]. For these applications, optical analysis is most promising because of its high sensitivity and short response time [3–5]. The use of laser light allows for particularly sensitive and specific detection. By using a laser as excitation source for fluorescent markers, spectral overlapping of the excitation light with the marker emission is avoided. To profit from these advantages in a LOC, external laser light can be coupled into the system. Nevertheless, coupling losses occur and alignment is critical. Alternatively, light sources are integrated in combination with passive photonic components and microfluidic structures. By integration of multiple detection units, parallel measurements on a single chip are possible. E.g., Balslev et al. [6] presented the integration of multiple photonic components including an optofluidic dye laser and embedded photodiodes into a LOC system. However, for bringing systems to market, fabrication costs need to be cut down, resulting in the demand for the use of low-cost

#141032 - $15.00 USD Received 12 Jan 2011; revised 16 Feb 2011; accepted 17 Mar 2011; published 14 Apr 2011

materials in a fabrication process suitable for mass production. Integrated organic optoelectronics and polymer photonics have gained interest in this respect as they offer a high potential to fulfill those requirements. In this context, polymer nanofibers were used to excite fluorescence in microchannels [7]. Furthermore, the integration of organic light emitting diodes (OLEDs) into microsystems was already investigated [8, 9]. The use of organic semiconductor lasers could combine the ease of processing of OLEDs with favorable emission properties of a laser. For this reason, the integration of organic lasers in combination with passive polymer optics was investigated [10, 11].

In this manuscript, a plastic LOC platform with integrated first order distributed feedback (DFB) organic semiconductor lasers (OSLs), deep ultraviolet (DUV) induced waveguides and microfluidic channels is presented. Chips of the platform are fabricated in a parallel four step process. We demonstrate that light of integrated lasers, coupled to waveguides, excites fluorescent markers in aqueous solution in a microfluidic channel.

The approach for the laser LOC platform is described at first. Subsequently, the fabrication and characterization of exemplary chips of this platform used for fluorescence excitation are discussed.

2. Platform description

The platform that is used for chips for fluorescence excitation here comprises a poly(methyl methacrylate) (PMMA) substrate with integrated lasers, waveguides and a microfluidic channel. A scheme of a chip is shown in Fig. 1a,b. It is sealed with a PMMA lid [12]. Substrate and lid consist of PMMA as this material can be micro- and nanostructered by thermal imprint. This allows for parallel generation of nanostructures for distributed feedback lasers and microfluidic structures in a single imprinting step [13]. PMMA is transparent for visible light. In contrast to this, exposure to DUV radiation causes breaking of the molecular chains in PMMA increasing its refractive index locally. Thus, by DUV exposure through a photomask waveguides are induced [14].

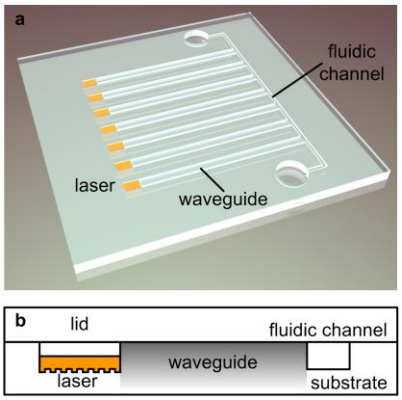

Fig. 1. (a) Scheme of an exemplary plastic LOC system with integrated lasers as used for fluorescence excitation and (b) sectional view of one detection unit on the same system (not to scale).

OSLs are integrated by evaporating a thin film of the organic semiconductor tris(8-hydroxyquinoline) aluminum (Alq_3) doped with the laser dye 4-dicyanomethylene-2-methyl-6-(p-dimethylaminostyril)-4H-pyrane (DCM) onto nanoimprinted first order DFB gratings. If a defined height of the thin film is selected it forms a single mode slab waveguide. Based on first order DFB, OSLs emit directed single mode polarized light in the chip plane. They feature a broad spectral tuning range [15, 16], low threshold [17], and are suitable for spectroscopic [18] or laser-induced fluorescence [19, 20] applications. OSLs must be pumped optically. While the readout system will require electrical and electronic components for operating the pumping laser source and processing the collected optical data, a disposable

#141032 - $15.00 USD Received 12 Jan 2011; revised 16 Feb 2011; accepted 17 Mar 2011; published 14 Apr 2011

chip itself will not include any electronic interface. Second order DFB lasers could be used on top of a microfluidic channel to excite fluorescence. However, the use of first order DFB lasers and waveguides is advantageous as the high energy pump laser light beam is geometrically separated from the interaction zone and does not have to be blocked by a filter. Additionally, the use of waveguides allows for local excitation in the microfluidic channel and facilitates the detection of fluorescence light.

OSL light is efficiently coupled into DUV induced waveguides on chip by introducing a topographical step [21]. To gain the coupling efficiency of light generated in the organic semiconductor laser into DUV induced waveguides the modes in an Alq_3:DCM slab waveguide and a DUV induced waveguide where calculated. The laser waveguide is an asymmetric slab waveguide on a PMMA substrate (refractive index of $n_s = 1.49$) with a core index of 1.74 and a cladding index of 1. An Alq_3:DCM height of 350 nm is assumed. The laser light is usually TE polarized as the threshold of TE modes is smaller as for the TM modes. A DUV exposure dose of 3 J/cm^2 results in a refractive index change at the PMMA surface of $\Delta n = 0.0075$. The index is exponentially decaying with the depth x according to $n = n_s + \Delta n \exp(x/d)$ for $x < 0$ with $d = 4.5$ µm. The waveguide surface subsides after DUV exposure and a small air gap remains after bonding depending on the process parameters. Simulations with the software BeamPROP™ have shown that modes for air gaps > 50 nm are the same as without a PMMA lid and that the field distribution in x direction at the waveguide center is independent of the waveguide width. Thus, the analytical method introduced by E. M. Conwell [22] can be used to calculate the field distribution in x direction with a cladding index of 1. The resulting fundamental TE modes of the laser slab waveguide and the DUV induced waveguide for a wavelength of 645 nm are plotted in Fig. 2a. The power coupling efficiency as function of the step height on the PMMA substrate can be calculated according to [23], Fig. 2b.

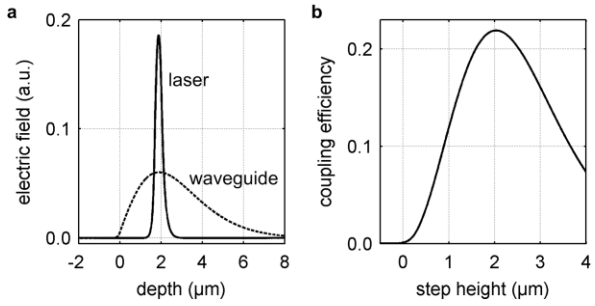

Fig. 2. (a) Slab waveguides modes of an organic semiconductor laser and a DUV induced waveguide. (b) Calculated coupling efficiency of both modes as function of the topographical step height on the PMMA substrate.

The laser light is guided to an interaction zone (i.e. at the crossings of waveguides and fluidic channel) where it can interact with an analyte inside a microfluidic channel. The fabrication process of the plastic chips consists of four main process steps: (1) combined thermal micro- and nanoimprint of the substrate topography, followed by (2) DUV exposure to induce waveguides and (3) evaporation of Alq_3:DCM on top of the DFB gratings through a shadow mask, and finally (4) thermal bonding of the lid to hermetically seal the lasers and close the microfluidic channel. On chips of the size of a microscope cover slip, the integrated components offer a variation of choices, e.g., the amount of waveguides and lasers, their width or the structure and topography of the microfluidic channels. The platform can thus easily be adapted to a desired application.

To demonstrate the functional capability of the platform for the on-chip excitation of fluorescent markers the following choices were made. λ/4 phase shifted linear first order DFB gratings [24] of 500 µm length and 300 µm width parallel to the grating lines in 1.6 µm deep basins of the same size were fabricated for the lasers. Grating periods of 190 nm to 215 nm in steps of 5 nm were chosen. At the same time a microfluidic channel of 0.1 mm width and

#141032 - $15.00 USD Received 12 Jan 2011; revised 16 Feb 2011; accepted 17 Mar 2011; published 14 Apr 2011

7.5 mm length was fabricated with a depth of 1.6 µm. Inside the channel linear gratings with a period of 460 nm were imprinted at the interaction zones to enhance the amount of fluorescent light directed to the detection system by Bragg scattering [25]. Waveguides of 300 µm width and 4.5 mm length are guiding the light of the lasers to the microfluidic channel.

3. Experimental

In the following, the fabrication of chips for fluorescence detection is described in detail. Characteristics of the optical setup and results of lasing and excitation of fluorescence in microfluidic channels are given.

3.1 Fabrication

At first, a silicon tool for replication was fabricated [12, 26]. On a 4" silicon wafer, gratings were made by electron beam lithography and subsequent aluminum deposition, lift-off, and reactive ion etching (RIE). An aligned UV lithography step on the same wafer was used for the fabrication of a resist mask for RIE of the microfluidic channel structure and the basins for the lasers respectively. After cleaning, deposition of an antistiction coating finished the tool. It was replicated into 0.5 mm thick semi finished HesaGlas® VOS substrates (acquired from Notz Plastics AG) by thermal imprint with a Jenoptik HEX 03 imprinting system. Therefore, a pressure of 2.65 MPa was applied at a temperature of 190°C for 15 min. After cooling, the stamp and the structured substrate were separated manually. Afterwards, waveguides were induced into the PMMA by aligned DUV exposure (240 – 250 nm) through a quartz chromium mask using a mask aligner (EVG 620) with a dose of 3 J/cm^2. A stencil shadow mask was fabricated by UV photolithography and electroplating of nickel. It was adjusted on top of the device. In a high vacuum chamber Alq_3 and 2.3% by weight of DCM were thermally co-evaporated up to a thickness of 350 nm. After removal of the mask, a 0.5 mm thick PMMA lid with prestructured inlets (diameter 1 mm) was bonded to the substrate at 78°C and 2.65 MPa under nitrogen atmosphere for 15 min using the imprinting system again. Finally, a wafer dicing saw separated the stack into chips of the size of microscope cover slips (18 × 18 mm^2) with ~1 mm thickness. A photograph of such a plastic chip is shown in Fig. 3. It additionally includes an atomic force micrograph of a DFB grating taken after thermal imprint and an optical micrograph of an interaction zone. The waveguide surface subsides after DUV exposure. Thus, waveguide and lid are not in intimate contact as can be seen in the micrograph due to the contrast and the appearing interference effects. To avoid leakage of an analyte onto the waveguide, a gap was left between waveguide and microfluidic channel.

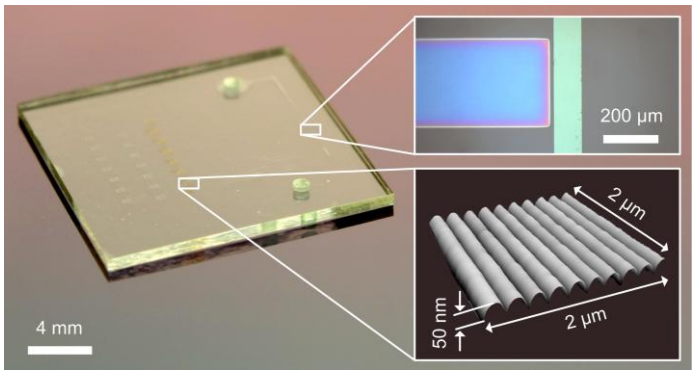

Fig. 3. Photograph of a plastic LOC system with an optical micrograph of an interaction zone (upper inset) and an atomic force micrograph of a DFB laser grating (lower inset).

#141032 - $15.00 USD Received 12 Jan 2011; revised 16 Feb 2011; accepted 17 Mar 2011; published 14 Apr 2011

3.2 Experimental setup

The experimental setup for the characterization of the chips is schematically depicted in Fig. 4. A UV laser (Newport, Explorer Scientific, EXPL-349-120-CDRH) emitting pulses of < 5 ns length at 349 nm is used as pump source. Utilizing a beam splitter and a calibrated photodiode the pump pulse energy is monitored during operation. The pump spot is focused to ~300 µm in diameter. Its size and position on the chip is controlled with a charge-coupled device (CCD) camera (Sony DXC-107A) behind the beam splitter (not shown in Fig. 4). To measure the optical signal from the interaction zones a microscope with a 20× objective with a numerical aperture of 0.42 is used. A second CCD camera (Starlight Xpress SXVF-H9) is mounted to the microscope in order to take images of the interaction zone. Alternatively, a multi mode optical fiber can be attached to examine spectral characteristics. The fiber leads to a spectrograph (Acton Research SpectraPro 300i, variable grating) connected to an intensified CCD camera (Princeton Research, PiMax 512). Two different long pass filters (Schott color glass filters RG645, RG665) are used to block light below ~645 nm or ~665 nm respectively. This arrangement blocks the laser light and only the excited fluorescent light is detected. Due to the polarized laser light blocking with a polarizer might be feasible as well, compare [7]. However, a spectral filter is used here as the exciting laser light and the fluorescence are spectrally separated due to the narrow laser line and the whole unpolarized fluorescent light can pass the filter. Both chip and microscope detection unit are mounted on separate xyz-translation-stages while the other components are fixed. By placing the microscope at the edge of the device, it can additionally be used to analyze the laser emission at the end facet with the spectrometer. In this case, a long pass filter blocking only the UV pump light is used. Capillary forces fill the microfluidic channels on the chips with the fluorescent solutions. The filling is accelerated by a low pressure applied with a miniaturized vacuum pump (Bürkert Micro Pump 7604) connected to one of the inlets.

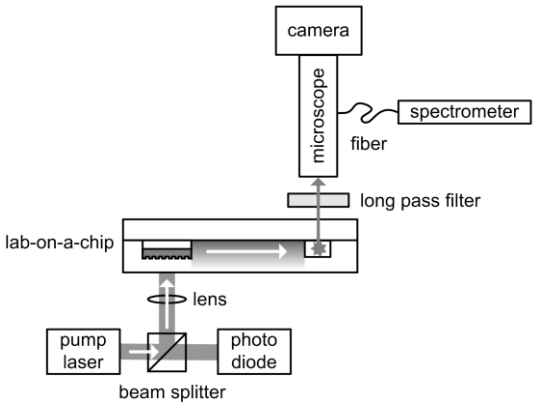

Fig. 4. Schematic illustration of the optical setup to prove the functional capability of fluorescence excitation on LOC systems.

3.3 Measurement results

At first, the integrated lasers were characterized using the pump laser and the spectrometer. Input-output curves were taken giving laser thresholds of typically ~0.7 µJ with the spot diameter being 300 µm. The threshold is increased due to absorption of the pump light by the substrate material [12]. Figure 5a exemplarily shows an input-output curve for a laser with a peak wavelength of 635 nm.

#141032 - $15.00 USD Received 12 Jan 2011; revised 16 Feb 2011; accepted 17 Mar 2011; published 14 Apr 2011

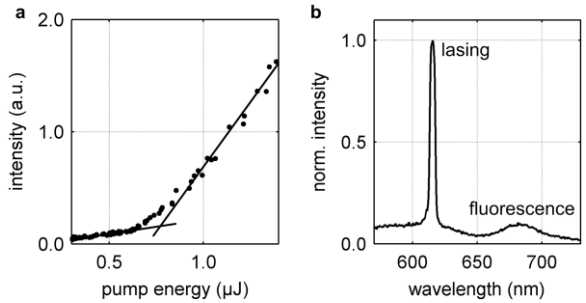

Fig. 5. (a) Input-output curve of an integrated laser and (b) laser and fluorescence spectrum taken at the interaction zone as shown in Fig. 4 without using a long pass filter to block the laser light.

In order to prove the functional capability of the device to excite fluorescent markers in aqueous solution microfluidic channels were filled with two different solutions: (1) carboxylate-modified microspheres (FluoSpheres®, dark red fluorescent, 660/680) of 0.04 μm in diameter mixed in aqueous solution to a concentration of 1% solids acquired from Sigma-Aldrich® and (2) goat anti-mouse IgG antibodies labelled with Alexa Fluor® 647 mixed in PBS buffer solution to a concentration of 2 mg/mL acquired from Invitrogen™. The absorption and the emission maximum of the FluoSpheres® are at 657 nm and 683 nm respectively and the same maxima are found for Alexa Fluor® markers at 650 nm and 671 nm respectively. Figure 5b shows a spectrum from an interaction zone taken with the setup shown in Fig. 4 without using a long pass filter. Therefore, the lasers were pumped with a repetition rate of 1 kHz and the fluorescence spectra were averaged by integrating over 20 s. The laser line is clearly visible on top of the fluorescence of the laser material as well as the excited fluorescence of the FluoSpheres®. However, for sensing with a simplified setup without a microscope and using a photodiode that does not distinguish between different wavelengths the light from the laser material must be blocked. Thus, the long pass filter blocking below ~665 nm was used. In Fig. 6a (left) a spectrum from an interaction zone is shown where the exciting laser light at 639 nm is blocked while the fluorescenct light passes the filter. The same is shown for the excitation of the Alexa Fluor® solution with laser light at 619 nm with a long pass filter blocking at ~645 nm, Fig. 6a (right). The observed noise in case of the Alexa Fluor® is stronger as compared to the FluoSpheres® measurement, which can be partially assigned to the exciting laser wavelength being further away from the absorption maximum of the Alexa Fluor® as in the case of the FluoSpheres®. Additionally, fluorescence light of the laser material overlaps with the light from the Alexa Fluor® markers, which is especially visible for shorter wavelengths were the fluorescence of DCM is stronger. By tuning the exciting laser wavelength to the maximum of the marker absorption the fluorescence of Alexa Fluor® can be enhanced [19]. Combined photographs of the interaction zone under illumination with a lamp and fluorescent light from FluoSpheres® taken with a CCD camera through the 665 nm long pass filter illustrate that the fluorescence is mainly detected from the edge of the microfluidic channel, Fig. 6b. This can be assigned to an exponential decay of the laser light intensity by absorption from the marker molecules and is consistent with results achieved with external lasers [27].

#141032 - $15.00 USD Received 12 Jan 2011; revised 16 Feb 2011; accepted 17 Mar 2011; published 14 Apr 2011

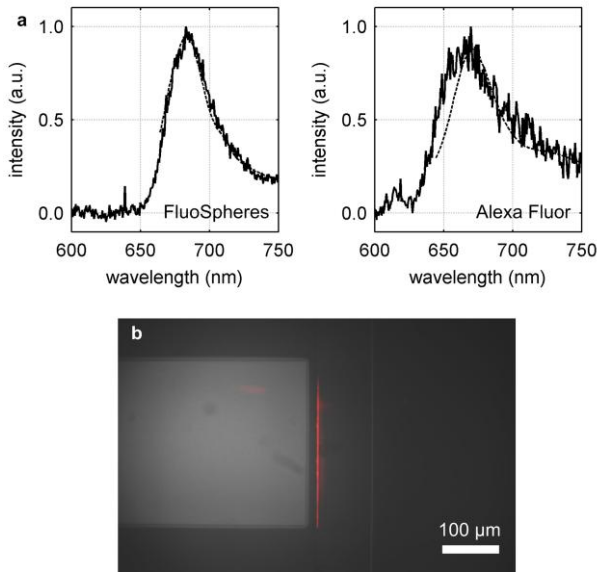

Fig. 6. Demonstration of fluorescence excitation. (a) Spectra of excited fluorescence in microfluidic channels (solid lines) and matched emission spectra of FluoSpheres® and Alex Fluor® (dashed lines). The laser light is blocked with long pass filters below ~665 nm in the case of the FluoSpheres® and below ~645 nm for Alexa Fluor®. (b) Combined photographs of interaction zone under illumination (grayscale) and fluorescent light from FluoSpheres® (red) taken with a CCD camera.

4. Conclusion

Future investigations on the presented platform will comprise time depended analysis and functionalization of the interaction zone enabling specific detection of more than one analyte component. E.g., lipid multilayers can be used to locally functionalize interaction zones or to form gratings for marker free detection [28]. Further, marker free detection schemes using interferometric devices [29] or the detection of shifts of photonic microcavity resonances [30–33] and plasmonic resonances [34] are feasible. Miniaturization of the surrounding reusable components and adaptation of the platform to specific applications will pave the way towards analysis in the field or at the point of care.

In summary, a plastic photonic lab-on-a-chip with integrated organic semiconductor lasers, waveguides, and a nanostructured microfluidic channel for exciting fluorescent markers used as labels for both, microspheres and antibodies, has been demonstrated here.

Acknowledgements

The kind support of Mads Brøkner Christiansen and Anders Kristensen of DTU Nanotech and Uwe Bog, Tobias Grossmann and Irina Nazarenko of the KIT is gratefully acknowledged. C. Vannahme and S. Klinkhammer are pursuing their Ph.D. within in the Karlsruhe School of Optics and Photonics (KSOP). The authors further acknowledge support by the Deutsche Forschungsgemeinschaft (DFG) and the State of Baden-Württemberg through the DFG-Center for Functional Nanostructures (CFN) within subproject A5.5. T. Mappes' Young Investigator Group received financial support from the "Concept for the Future" of the KIT within the framework of the German Excellence Initiative.

#141032 - $15.00 USD Received 12 Jan 2011; revised 16 Feb 2011; accepted 17 Mar 2011; published 14 Apr 2011